ABCM

TURBULENT WATER CHANNEL FLOWS UNDER SURFACE WIND ACTION

Jucá, P.C.S. and Maliska, C.R.
Computational Fluid Dynamics Laboratory - SINMEC
Department of Mechanical Engineering - UFSC
88040-900 - Florianópolis - SC - Brazil

SUMMARY

This work reports the last improvements and tests in a numerical model designed to simulate the circulation and pollutant transport in water bodies and coastal waters. The introduction of a $\kappa - \varepsilon$ turbulence model in the numerical model and the ability to incorporate surface winds conditions acting over the dispersion plumes are related and tested against experiments.

INTRODUCTION

Water is one of the basic natural resources of human being. The conservation and protection of our environment is therefore of great importance to our well-fare or even to our existence. Industrialization, besides the social progress, produce huge quantities of waste materials to be disposed of, so sewage discharges are significant pollutant sources for many urban estuaries and coastal areas. In particular, if sufficient rain storm occurs, municipal and industrial sewage discharges may exceed the capacity of existing wastewater treatment plant and discharge directly to the surface of the receiving water bodies.

To understand the circulation and pollutant transport in water bodies and coastal waters several numerical techniques have been developed in the last two decades. Most recently 3D numerical models have been implemented with different degrees of complexity in order to simulate more accurately the physical phenomena involved in this kind of problem, as can be seen in Fisher (1981), Jin (1993) and Huang and Spaulding (1995), among others.

In the scope of this research project Maliska et all (1987) proposed a 2D model for surface discharge using boundary-fitted grids. Following, Jucá et all (1989), reported a 3D model also using generalized coordinates. Recently, Jucá (1994) presented a complete 3D model for thermal and pollutant dispersion.

The present work reports the last improvements in the numerical model, where a κ-ε turbulence scheme was incorporated to the original model (Jucá and Maliska, 1995). To validate it, a rectangular channel flow with a surface wind was simulated and compared with the experiments of Yu (1987).

THE MATHEMATICAL MODEL

Due to the irregular shapes of general water bodies, the discretization employed is self-conforming to the boundaries. If an structured grid is used, as in this work, the governing equations are easily managed using a coordinate transformation. Using ϕ to represent any of the dependent variables, the general conservation equation can be written as

$$\frac{1}{J}\frac{\partial(\rho\phi)}{\partial t} + \frac{\partial}{\partial\xi}(\rho U\phi) + \frac{\partial}{\partial\eta}(\rho V\phi) + \frac{\partial}{\partial\gamma}(\rho W\phi) = -\hat{P}^{\phi} + \hat{S}^{\phi}$$
$$+ \frac{\partial}{\partial\xi}\left[\left(\alpha_{11} J\Gamma\frac{\partial\phi}{\partial\xi}\right) + \left(\alpha_{12} J\Gamma\frac{\partial\phi}{\partial\eta}\right) + \left(\alpha_{13} J\Gamma\frac{\partial\phi}{\partial\gamma}\right)\right] \quad (1)$$
$$+ \frac{\partial}{\partial\eta}\left[\left(\alpha_{21} J\Gamma\frac{\partial\phi}{\partial\xi}\right) + \left(\alpha_{22} J\Gamma\frac{\partial\phi}{\partial\eta}\right) + \left(\alpha_{23} J\Gamma\frac{\partial\phi}{\partial\gamma}\right)\right]$$
$$+ \frac{\partial}{\partial\gamma}\left[\left(\alpha_{31} J\Gamma\frac{\partial\phi}{\partial\xi}\right) + \left(\alpha_{32} J\Gamma\frac{\partial\phi}{\partial\eta}\right) + \left(\alpha_{33} J\Gamma\frac{\partial\phi}{\partial\gamma}\right)\right]$$

where U,V,W are the contravariant components of the velocity given by:

$$U = (u_1\xi_x + u_2\xi_y + u_3\xi_z)\,J^{-1}$$
$$V = (u_1\eta_x + u_2\eta_y + u_3\eta_z)\,J^{-1} \quad (2)$$
$$W = (u_1\gamma_x + u_2\gamma_y + u_3\gamma_z)\,J^{-1}$$

where the α_{ij} are the components of the metric tensor and J the jacobian of the coordinate transformation. As stated, ϕ represents the dependent variables for each equation. For $\phi = 1, u_1, u_2, u_3$, the mass conservation equation, momentum in x, y and z Cartesian coordinates directions, are recovered, respectively. Γ represents the diffusivity transport coefficient, being zero for the mass conservation equation and equals to the effective viscosity for the Navier-Stokes equations. Also in Eq. (2) u_i represents the mean of fluctuating Cartesian velocities as defined by Rodi (1980). Details of the coordinate transformation can be found in Maliska (1995).

The term P^{ϕ} is zero for the mass conservation equation. For the Navier-Stokes equations it is the pressure term given by

$$\hat{P}^{u_i} = \left[\frac{\partial p}{\partial\xi}\bar{\xi}_i + \frac{\partial p}{\partial\eta}\bar{\eta}_i + \frac{\partial p}{\partial\gamma}\bar{\gamma}_i\right] \quad (3)$$

where the subscript indicates partial derivative in the "i-th" Cartesian direction. The source term S^{ϕ} is zero for mass conservation equation and for the Navier-Stokes equations it is written as

$$\hat{S}^{u_i} = \frac{\partial}{\partial\xi}\left[\left(J\mu_{ef}\frac{\partial U}{\partial\xi}\right)\bar{\xi}_i + \left(J\mu_{ef}\frac{\partial U}{\partial\eta}\right)\bar{\eta}_i + \left(J\mu_{ef}\frac{\partial U}{\partial\gamma}\right)\bar{\gamma}_i\right]$$
$$+ \frac{\partial}{\partial\eta}\left[\left(J\mu_{ef}\frac{\partial V}{\partial\xi}\right)\bar{\xi}_i + \left(J\mu_{ef}\frac{\partial V}{\partial\eta}\right)\bar{\eta}_i + \left(J\mu_{ef}\frac{\partial V}{\partial\gamma}\right)\bar{\gamma}_i\right] \quad (4)$$
$$+ \frac{\partial}{\partial\gamma}\left[\left(J\mu_{ef}\frac{\partial W}{\partial\xi}\right)\bar{\xi}_i + \left(J\mu_{ef}\frac{\partial W}{\partial\eta}\right)\bar{\eta}_i + \left(J\mu_{ef}\frac{\partial W}{\partial\gamma}\right)\bar{\gamma}_i\right]$$

Eq. (1), representing the system of partial differential equations governing the channel flow, is integrated in time and in a 3D elemental control volume. The pressure-velocity coupling is handled using the SIMPLEC method of Van Doormaal and Raithby, (1984). Fictitious control volumes are used for the application of the boundary conditions. The resulting linear system of equations are of the form:

$$\begin{aligned} A_p\phi_p &= A_e\phi_E + A_w\phi_W + A_n\phi_N \\ &+ A_s\phi_S + A_d\phi_D + A_f\phi_F \\ &+ A_{ne}\phi_{NE} + A_{se}\phi_{SE} + A_{nw}\phi_{NW} \\ &+ A_{sw}\phi_{SW} + A_{de}\phi_{DE} + A_{fe}\phi_{FE} \\ &+ A_{dw}\phi_{DW} + A_{fw}\phi_{FW} + A_{dn}\phi_{DN} \\ &+ A_{ds}\phi_{DS} + A_{fn}\phi_{FN} + A_{fs}\phi_{FS} + b_p \end{aligned} \quad (5)$$

for $\phi = 1, u_1, u_2, u_3$. An equation for pressure is derived from the mass conservation equation using the SIMPLEC method. Due to the 3D nature of the problem, numerical details and expressions of the coefficients are not given. These can be found in Jucá, (1994), Marchi, (1992) and Maliska, (1995). To deal with turbulent flows a κ–ε turbulence model was implemented. So, in Eq. (1) the effective viscosity are defined by $\mu_{ef} = \mu_t + \mu_l$, where μ_{ef} μ_t and μ_l are the effective, turbulent and laminar viscosity, respectively. The turbulent viscosity is given by

$$\mu_t = \rho C_\mu \frac{\kappa^2}{\varepsilon} \quad (6)$$

where $C_\mu = 0.09$, ρ is the density of the water and κ and ε are the turbulent kinetic energy and its turbulent dissipation, respectively. The transport equations for κ and ε also can be obtained from Eq. (1). For this, ϕ is made equal to κ and ε. The terms $\tilde{P}^\phi$ are given by

$$\tilde{P}^\kappa = \tilde{P}^\varepsilon = 0 \quad (7)$$

for κ and ε. The source $\tilde{S}^\phi$ terms are

$$\tilde{S}^\kappa = \rho\tilde{P}_{dt} - \rho\varepsilon \quad ; \quad \tilde{S}^\varepsilon = \rho\left(C_{1\varepsilon}\frac{\varepsilon}{\kappa}\tilde{P}_{dt} - C_{2\varepsilon}\frac{\varepsilon^2}{\kappa}\right) \quad (8)$$

The values for the constants are taken the usual ones recommended in literature, $C_{1\varepsilon} = 1{,}44$ and $C_{2\varepsilon} = 1{,}92$. These are current values used in this kind of flows as can be seen in Rodi (1980) and Huang and Spaulding, (1995). The production term $\tilde{P}_{dt}$ in the transformed space is written as

$$\begin{aligned} \tilde{P}_{dt} = J\mu_{ef}\{ & 2\left[\left(\frac{\partial u}{\partial\xi}\right)\bar{\xi}_x + \left(\frac{\partial u}{\partial\eta}\right)\bar{\eta}_x + \left(\frac{\partial u}{\partial\gamma}\right)\bar{\gamma}_x\right]^2 \\ & + 2\left[\left(\frac{\partial v}{\partial\xi}\right)\bar{\xi}_y + \left(\frac{\partial v}{\partial\eta}\right)\bar{\eta}_y + \left(\frac{\partial v}{\partial\gamma}\right)\bar{\gamma}_y\right]^2 \\ & + 2\left[\left(\frac{\partial w}{\partial\xi}\right)\bar{\xi}_z + \left(\frac{\partial w}{\partial\eta}\right)\bar{\eta}_z + \left(\frac{\partial w}{\partial\gamma}\right)\bar{\gamma}_z\right]^2 \\ & + \left[\frac{\partial}{\partial\xi}(u\bar{\xi}_y + v\bar{\xi}_x) + \frac{\partial}{\partial\eta}(u\bar{\eta}_y + v\bar{\eta}_x) + \frac{\partial}{\partial\gamma}(u\bar{\gamma}_y + v\bar{\gamma}_x)\right]^2 \\ & + \left[\frac{\partial}{\partial\xi}(u\bar{\xi}_z + w\bar{\xi}_x) + \frac{\partial}{\partial\eta}(u\bar{\eta}_z + w\bar{\eta}_x) + \frac{\partial}{\partial\gamma}(u\bar{\gamma}_z + w\bar{\gamma}_x)\right]^2 \\ & + \left[\frac{\partial}{\partial\xi}(v\bar{\xi}_z + w\bar{\xi}_y) + \frac{\partial}{\partial\eta}(v\bar{\eta}_z + w\bar{\eta}_y) + \frac{\partial}{\partial\gamma}(v\bar{\gamma}_z + w\bar{\gamma}_y)\right]^2 \} \end{aligned} \quad (9)$$

The diffusivity transport coefficient Γ for the κ-ε turbulence model, see Eq (1), are given by

$$\Gamma^\kappa = \frac{\mu_t}{\sigma_k} \quad ; \quad \Gamma^\varepsilon = \frac{\mu_t}{\sigma_\varepsilon} \quad (10)$$

where the constants have the values of $\sigma_\varepsilon = 1.30$ e $\sigma_\kappa = 1.0$

BOUNDARY CONDITIONS

Typically, in an environmental flow we have solid boundaries represented by the shoreline and by the bottom of the water body. At the surface the wind acts over the dispersion of the pollutant plume causing its superficial spreading and / or bending. For solid and surface boundaries no normal flux of momentum is allowed. The turbulent stresses at the solid boundaries, σ_b , are determined by

$$\sigma_b = \frac{k_v v_b}{\ln\left(\frac{\Delta Z_b}{Z_0}\right)} \quad (11)$$

where v_b is the component of the velocity *parallel to the boundary* $k_v = 0.41$ is the Von Karman constant; ΔZ_b the distance from the boundary to the nearest grid point and Z_0 a parameter dependent on the local boundary roughness, Jin (1993), assuming hydraulically smooth flow. Eq. (11) indeed assumes that the velocity near the solid boundaries matches the logarithmic law of the wall, and for that, sufficient mesh resolution must be provided near the boundary. At the surface the wind stress is often calculated by (Huang and Spaulding, 1995)

$$\sigma_w = \rho_w C_d v_{wind}^2 \quad (12)$$

where C_d is the air-water drag coefficient, ρ_w the air density and v_{wind} it's velocity, measured at 10 m. height. In the present work, the stresses due to wind are know from experimental data.

The stresses at the boundary imposes the boundary conditions for the velocity. As a simple example, if the plane xy is parallel to the surface and bottom, and z is the depth direction of the water body, the bottom stress there can be approximated by

$$\sigma_{ib} = \mu_{ef}\left(\frac{u_{ib} - u_{ip}}{2Z_p}\right) \qquad (13)$$

where "i" represents the "i-th" Cartesian direction (i = 1,2).

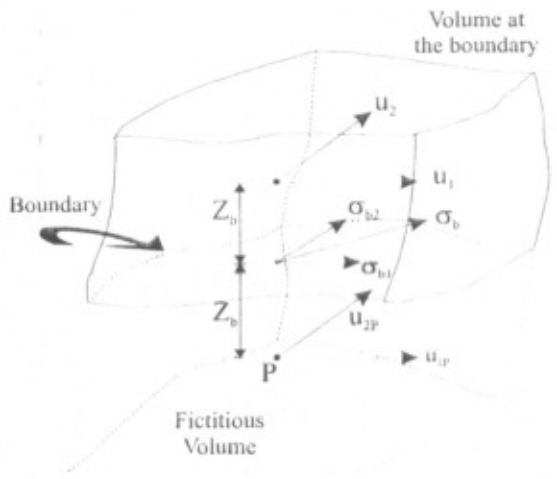

Fig 1 - Turbulent tension sketch at the boundary

Rewriting

$$u_{ip} = u_{ib} - \left(\frac{2Z_p\sigma_{ib}}{\mu_{ef}}\right) \qquad (14)$$

which imposes the boundary conditions for the velocity. The turbulent kinetic energy and its dissipation at solid boundaries are determined following Rodi (1980), as

$$\kappa_b = \frac{v_*^2}{(C_\mu)^{0.5}} \quad ; \quad \varepsilon_b = \frac{v_*^3}{k\Delta Z} \qquad (15)$$

At the bottom the resulting shear velocity is

$$v_* = \sqrt{\frac{(\sigma_{1b}^2 + \sigma_{2b}^2)^{0.5}}{\rho}} \qquad (16)$$

where v_* is the friction velocity at the bottom. With the surface stress the κ and ε values at the surface can be calculated using Eq. (15)

MODEL VERIFICATION

Comparisons of the mathematical model against analytical or experimental results are a necessary step in any model development.

In this work it was chose to compare the proposed model with a systematic experimental study of turbulent channel flows induced by wind at the free surface carried out by Yu (1987) as partially related in Jin (1993). The experiment was realized in a flume 38 m long, with a cross section of 0.80 m x 0.59 m, as show in Fig. 2. The flume was provided with a roof, a suction ventilator at one end of the flume and an air intake at the other end. So, a driving air current could be created. The velocity of the air current (u_a) was measured 10 cm above the water surface and ranged from 3.7 m/s to 8.0 m/s during the experiment.

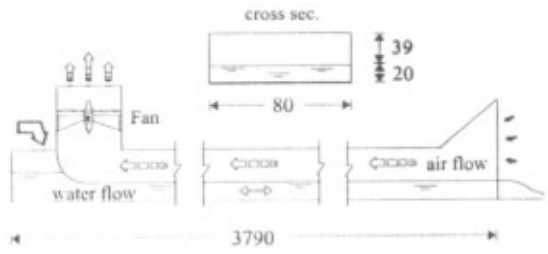

Fig. 2 - Experimental apparatus of Yu (1987). Dimensions in cm.

The still water depth (D) was maintained at 20 cm. Steady water flows was created using a pump with mean cross-sectional velocities varying from 4.75 cm/s to 21.4 cm/s. The flow in the water could be in a direction either following the wind or opposing it and the test section was located near the middle of the flume where the depth was little affected by wind-setup of the free surface. The bottom of the flume was made of cement and all flow tests were found to be in the hydraulic smooth regime $k_v = 0.41$ is the Von Karman constant; ΔZ_b the distance from the boundary to the nearest grid point and Z_0 a parameter dependent on the local boundary roughness..

Using the measurements of the centerline velocity profiles, Yu proposed two logarithmic profiles, one for the flow near the surface and another for the flow near the bottom. Upon examining these formulations Yu obtained the values of the surface friction velocity (u_s^*) and the equivalent bottom roughness height (Z_0) by means of the profile method. Table 1 shows the conditions of typical experimental runs choose to compare against the mathematical model proposed.

Table 1 - Experimental data from Yu (1987)

Run	$\bar{u}_w$	u_a	u^*_s	Z_0
	cm/s	m/s	cm/s	mm
1	5,0	-5,70	0,929	0,2570
2	10,40	-5,70	0,856	0,0553
3	14,10	-5,70	0,852	0,0486
4	18,00	-5,70	0,895	0,0491
5	10,40	8,00	1,016	0,3790
6	14,10	8,00	0,993	0,1340
7	18,00	8,00	1,010	0.0187
8	21,40	8,00	1,010	0.0268

In Tab. 1 the signal (-) in the velocity of the air (u_a) means it is blowing against the water flow.

It is important to note that the mean water velocity reported in Jin (1993) **is not** the experimental flow rate over the entire cross section, as a first reading of his work suggests. The mean water velocity in Table 1 is obtained by integrating the experimental center velocity profile over the channel depth only. In other words, it is the average of an infinitely large channel where the side walls have no influence in the velocity profiles. This fact was confirmed by adjusting a 4th degree polynomial curve to the experimental points and performing the integral over

the depth which leads to the mean water velocities listed in Table 1.

NUMERICAL SIMULATION OF THE CHANNEL FLOW

Two simulations of the channel flow were performed. The first one for comparing the model against the available experimental results. In this one the channel was considered infinitely large so the data in Table 1 is well suited. In the second case the side wall were considered in order to appreciate the performance of the mathematical model when more than one solid boundary were present and a fully 3D flow exists.

For the large channel, symmetry boundary conditions were applied in the north and south boundaries, as show in Fig 3.

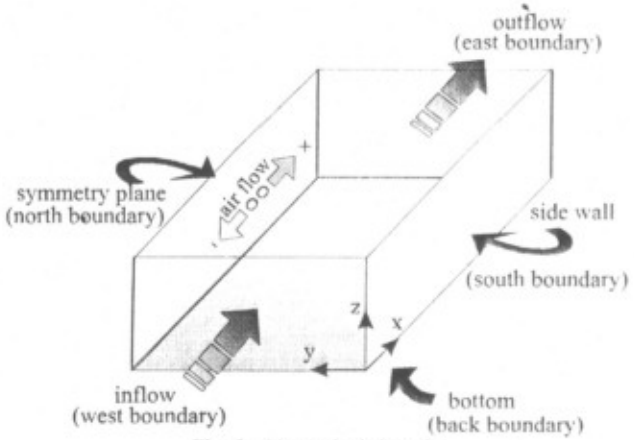

Fig. 3 - Numerical domain

In the west face, the inflow boundary condition applies in all cases. Since no information about the inlet velocity profile in the flume where available, an uniform velocity profile ($\bar{u}_w$) was imposed. For the turbulent kinetic energy and its dissipation, boundary conditions as proposed by Demuren and Rodi (1983) were taken

$$\kappa = 0.004\, u_{in}^2 \qquad ; \qquad \varepsilon = C_\mu \frac{\kappa^{1.75}}{0.09\, b} \tag{17}$$

where b is the channel width. At the east boundary a parabolic boundary condition were applied for all variables. Therefore

$$\frac{\partial \phi}{\partial \xi} = 0 \qquad \text{for} \quad \phi = u_i\ ,\kappa\ ,\varepsilon \tag{18}$$

At the bottom and at the surface of the water (front and back), and at the south wall (in the second case), the boundary conditions for velocities were applied as described in Eq (14). For κ–ε the boundary conditions are taken from Eq (15) with the friction velocity from Table 1 at the surface, and from Eq (11) and Eq (15) for solid boundaries.

For the infinitely large channel case, the domain discretization were made with a rectangular Cartesian mesh with 80x5x21 (x,y,z) volumes. In all cases, for numerical computations, half of channel width were taken due to the symmetry of the flow (15,0x0,4x0,2 m.). In the case were there exists the lateral wall (south face) a Cartesian regular mesh of 80 x 15 x 21 volumes (x, y, z) volumes where used.

RESULTS

Figure 4 and 5 depicts the center line vertical velocity (u_1) profile against the experimental measurements of Yu (1987).

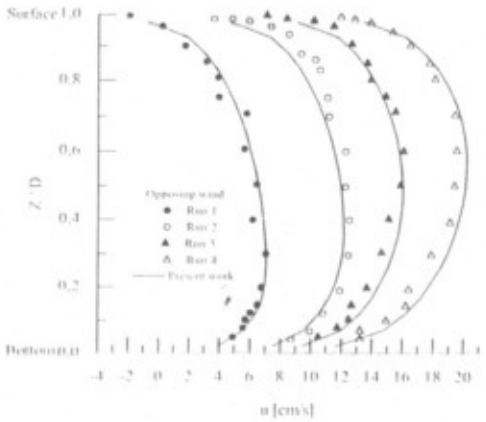

Fig. 4 - Center line vertical profile. Opposing wind cases

As could be observed by the numerical results, at the section test the profile was fully developed for all run cases in table 1.

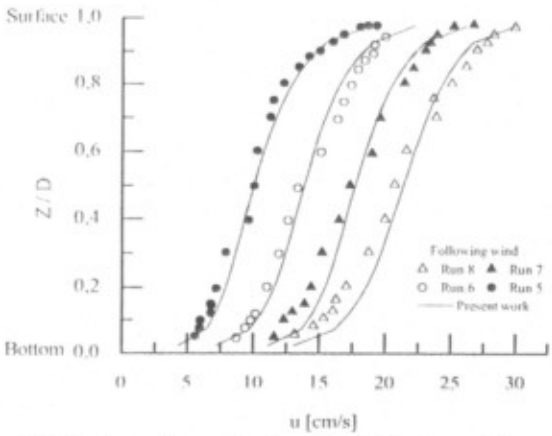

Fig.5 - Center line vertical profile. Following wind cases.

The numerical results show a very good agreement with the experimental measurements, pointing out that the proposed mathematical modeling suits well for channel flows, considering the κ–ε turbulence model equations.

In the opposing wind cases is interesting to note the run 1 where the velocity at the surface is against the direction of flow imposed at inflow boundary. In the remaining cases the opposing wind acts like a wall with different roughness values, retaining the velocity profile at the surface.

Jim (1993) used 2D κ–ε model for modeling the channel flow as reported in case one. For some runs he reported the μ_{ef} profiles. These profiles are show in Fig 6 against the resulting profiles obtained in the present work for the large channel case.

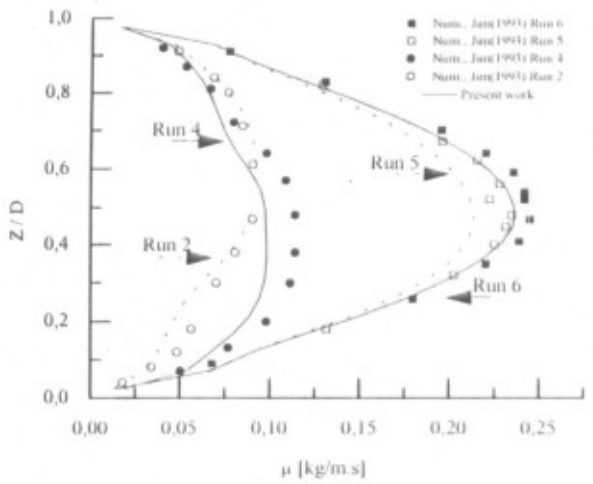

Fig 6 - Effective viscosity profiles

The resulting numerical μ_{ef} profiles are quite similar and show a good agreement, mainly if considered that the $\kappa-\varepsilon$ model was applied under different hypothesis for Navier-Stokes equations and solution methods.

Figure 7 depicts the center line vertical velocity u_l profile for the second case were the lateral (south) wall is present. In this case the channel flow is better simulated, as soon as the influence of the wall is taken over the velocity profiles. This is more close to the reality of low aspect ratios channels. The shape of the curves are similar to the ones of case 1 however there are no experimental results available to comparisons.

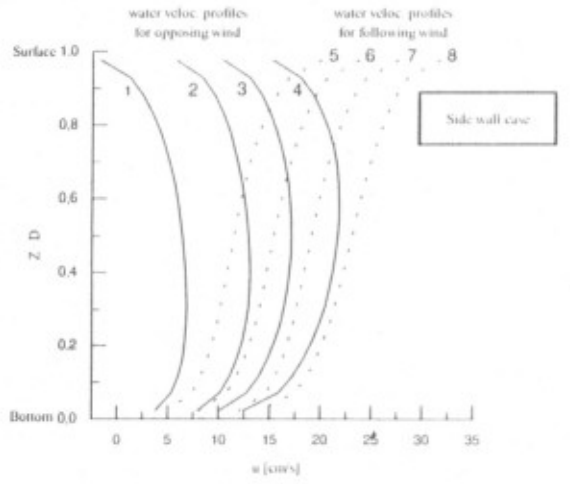

Fig. 7 - Velocity profiles for the finite channel case.

As in the preceding case, in the run 1, the resulting surface velocity is against the imposed water profile in west boundary, although the reverse flow is lower. It's due the presence of the lateral wall that leads to great velocity profiles in the center line, lowering the reversal flow caused by the wind.

Figure 8 present the μ_{ef} profile for the same runs presented before, but for the wall channel case. Comparison between Fig 8 and 6 show that, as expected, the profiles are similar but larger values of μ_{ef} are present.

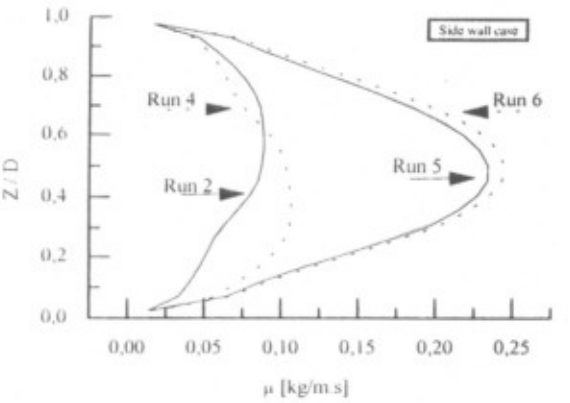

Fig.8 - Effective viscosity profiles for the side wall case.

CONCLUSION

Due the agreement of the numerical results with the experimental data available for the channel flows under different flow rates and wind situations we can conclude that the mathematical modeling is well suited for the physics analyzed.

To reach the final goal of the model a conservation equation for chemical species or energy conservation equation will be soon incorporated in order to simulate pollutant dispersion or heat discharges in water bodies and coastal water.

The overall agreement of the velocity profiles comparisons also shows that the boundary conditions are appropriate and its implementation is correct.

REFERENCES

Demuren, A .O. , Rodi, W., 1983, "Side Discharges into Open Channels: Mathematical Models", J. Hydr. Eng., ASCE, 109(12), pp. 1707-1722

Van Doormaal, J.P., Raithby, G.D., 1984, "Enhancements of the SIMPLE Method for Predicting Incompressible Flúid Flow", Num. Heat Transfer, vol. 7 pp. 147-163

Fisher, H.B., 1981, "Transport Models for Inland and Coastal Waters", New York, Academic Press, 542 pp., Proceedings of a Symposium on Predictive Ability.

Huang, W., Spaulding, M., 1995, "3D Model of Estuarine Circulation and Water Quality Induced by Surface Discharges", Journal of Hydraulic Eng., vol. 121, No 4, pp. 300-311.

Jin, X.Y., 1993, "Quasi-Tridimensional Numerical Modeling of Flow and Dispersion in Shallow Water", Communication on Hydraulic and Geotechnical Engineering, Dp of Civil Eng., Delft Univ. of Technology, Rep. 93-03, ISSN 0169-6548.

Jucá, P.C.S., Silva, A.F.C., Maliska, C.R.,1989, "Solução Numérica de Problemas Tridimensionais Elípticos de Convecção de Calor", X Congresso Brasileiro de Engenharia Mecânica, pp. 161-164, Rio de Janeiro, Brazil

Jucá, P.C.S., 1994, "Modelagem Tridimensional Turbulenta da Dispersão de Poluentes em Corpos D'água de Geometria Variável", Exame de Qualificação do Curso de Pósgraduação em Engenharia Mecânica, UFSC, Centro Tecnológico; Universidade Federal de Santa Catarina

Jucá, P.C.S., Maliska, C.R ,1995, "Tridimensional Simulation of Pollutant Dispersion in Water Bodies", XVI Congresso Íbero Americano sobre Métodos Computacionais para Engenharia, vol. 1, pp. 640-649.

Maliska, C.R., Silva, A.F.C., Polina, S., Perez, J.A.O., 1987, "Heat Transfer Predictions of Thermal Discharges in Water Bodies", IX Congresso Brasileiro de Engenharia Mecânica, pp. 45-48, Florianópolis, SC, Brazil

Maliska, C.R., 1995, "Transferência de Calor e Mecânica dos Fluidos Computacional: Fundamentos e Coordenadas Generalizadas", Livros Técnicos e Científicos Editora

Marchi, C.H., 1992, "Solução Numérica de Escoamentos Tridimensionais Viscosos em Qualquer Regime de Velocidade", Dissertação de Mestrado, Curso de Pós-Graduação em Engenharia Mecânica, Departamento de Engenharia Mecânica, Centro Tecnológico, Universidade Federal de Santa Catarina

Rodi, W., 1980, "Turbulence Models and Their Application in Hydraulics", Int. Assoc. for Hydraulic Research , Delft, Netherlands.

Yu, X., 1987, "Turbulent Channel Flow under the Action of Surface Wind Stress", Internal Report No 2-87, Lab. Of Fluid Mechanics , Dpt of Civil Engineering, Delf Univ. of Technology.